

# Cloud Generation Using a Huge Vertical Mine

Chang-Jin Ma\*

*Department of Environmental Science, Fukuoka Women's University, Fukuoka, Japan*

(Received 14 September 2006, accepted 20 December 2006)

## Abstract

In order to study the characteristics of cloud, a real-scale experiment for cloud generation was carried out using an extinct vertical mine (430 m height) located in the northeastern Honshu, Japan. The dry particles generated from the three-step concentrations of NaCl solutions were used for cloud generation. The number size distributions of initial dry particles and cloud droplets were monitored by Scanning Mobility Particle Sizer (SMPS) and Forward Scattering Spectrometer Probe (FSSP) at bottom and upper sites of pit, respectively. The polymeric water absorbent film (PWAFF) method was employed to measure liquid water content ( $W_L$ ) as a function of droplet size. Moreover the chemical properties of individual droplet replicas were determined by micro-PIXE. The CCN number concentration shows the lognormal form in dependence of the particle size, while the number size distributions of droplets are bimodal showing the peaks around 9  $\mu\text{m}$  and 20  $\mu\text{m}$  for every case. In comparison to background mineral particles, right shifting of size distribution line for NaCl particles was occurred. When NaCl solutions with three-step different concentrations were nebulized,  $W_L$  shows the strong droplet size dependence. It varied from 10.0  $\text{mg m}^{-3}$  up to 13.6  $\text{mg m}^{-3}$  with average 11.6  $\text{mg m}^{-3}$ . A good relationship between  $W_L$  and cloud droplet number concentration was obtained. Both chemical inhomogeneities (mixed components with mineral and Cl) and homogeneities (only mineral components or Cl) in individual droplet replicas were obviously observed from micro-PIXE elemental images.

**Key words :** Cloud, Droplet replica, CCN, Liquid water content, Micro-PIXE

## 1. INTRODUCTION

Aerosols that serve as the nuclei upon which water vapor condenses in the atmosphere are called cloud condensation nuclei (CCN). Homogeneous nucleation of condensation is the formation of pure water droplets by condensation from a supersaturated vapor without the aid of aerosols. Water droplets in warm clouds form by what is known as

heterogeneous nucleation on atmospheric aerosols. The nucleation scavenging of aerosols in clouds refers to activation and subsequent growth of a fraction of the aerosol population to cloud droplets. Aerosol activation depends on aerosol number concentration, updraft velocity, mean radius and standard deviation of aerosol size distribution, aerosol composition, air temperature, and atmospheric pressure.

Clouds are a major factor in the Earth's radiation budget, reflecting sunlight back to space or blanketing the lower atmosphere and trapping infrared radiation emitted from the Earth's surface. Also the

\* Corresponding author. Tel : +81-92-661-2411(ext. 373),  
Fax : +81-92-661-2415, E-mail : ma@fwu.ac.jp

properties of aerosols in cloud have an influence on different heating/cooling rates. Twomey *et al.* (1984) pointed out that the effect of anthropogenic CCN on climate could be an extremely important climatic factor which could in fact be of the same magnitude as the “greenhouse effect” of increased concentrations of trace gases (mainly carbon dioxide). Kim and Kwon (2006) carried out the study of aerosol indirect effect by using the ground-based remote sensing. The ability of a given particle to serve as a nucleus for water droplet formation will depend on its size, chemical composition, and the local supersaturation. Thus, to know the characteristics of cloud is one of key issues in understanding the cloud scavenging mechanism as well as the Earth’s radiation budget.

A large number of numerical studies on CCN and its effect to cloud droplets have been made (Kwak *et al.*, 1990; Kuba and Takeda, 1983; Lee *et al.*, 1980). Also numerous experimental attempts have been made to study the cloud chemistry and physics (Gurciullo and Pandis, 1997; Ratzel and Constantineau, 1990; Garvey, 1975). However, only few attempts have so far been made to study cloud properties at field experiments by the real scale cloud generation.

The primary objective of the present study is to establish the relationships among chemistry and sources of CCN, cloud droplet concentration and size distribution, and  $W_L$ . Here, the physical properties of cloud artificially generated at a huge vertical chamber are reported. The cloud chemical characteristics concentrated on individual cloud droplets are also described.

## 2. MATERIAL AND METHODS

### 2.1 Description of vertical mine chamber

In this study, to investigate the characteristics of cloud a huge vertical mine located in Kamaishi City, Japan was employed for cloud generation experiment. Kamaishi City is situated in the southeastern section of Iwate prefecture, Japan. Since a big amount of steel including iron is deposited

nearby this city, the iron industry has played a central part in Kamaishi City. Kamaishi City has been called as the birthplace of Japan’s modern iron industry. A huge vertical pit employed as the real-scale chamber for artificial cloud generation in this study is also one of the extinct iron-copper mines located at steep mountains and valleys. In comparison to coalmine, this vertical iron-copper mine has the very stable four-side walls without any entrance of artificial particles.

The schematic view of the vertical mine chamber is illustrated in Fig. 1. Also photographs of aerosol generation, impactor sampler system, and cloud water collector are displayed in Fig. 1. This extinct mine consists of a vertical pit with 430 m height and  $5.5 \times 2.9 \text{ m}^2$  cross sectional area. There are two entrances at the top and bottom of pit. In order to prevent the entrainment of dry air and external particles, these horizontal entrances are blocked during experiment. Since upward motion of moist air is an essential prerequisite for cloud formation, air parcel should be lifted to top of pit. The ascending air parcel wind speed was controlled by two large ventilators at the top of pit (see Fig. 1). The wind speed of ascending air parcel was varied 0.8 to  $1.9 \text{ m s}^{-1}$ . Even though the external air was isolated during experiment, the ascending air parcel through the vertical pit was possible. Because so many other branches of mine are connected to a vertical pit, the internal air can be circulated.

Also due to the subterranean water, the atmosphere of vertical mine is always wetted with relative humidity near 100%. Thus background cloud is always forming. Average temperature at bottom and upper sites are  $13.2^\circ\text{C}$  and  $11.3^\circ\text{C}$ , respectively.

### 2.2 Instrumentation

The polydisperse dry particles were generated from the three-step concentrations of NaCl solutions by an atomizer (TSI 3076) at bottom of pit. Considering the wind speed of ascending air parcel and the height of vertical pit is critical for the decision of duration time of CCN dispersion at the inlet of a vertical pit. The necessary time that air parcel can be arrived at upper site passing through a cylindrical

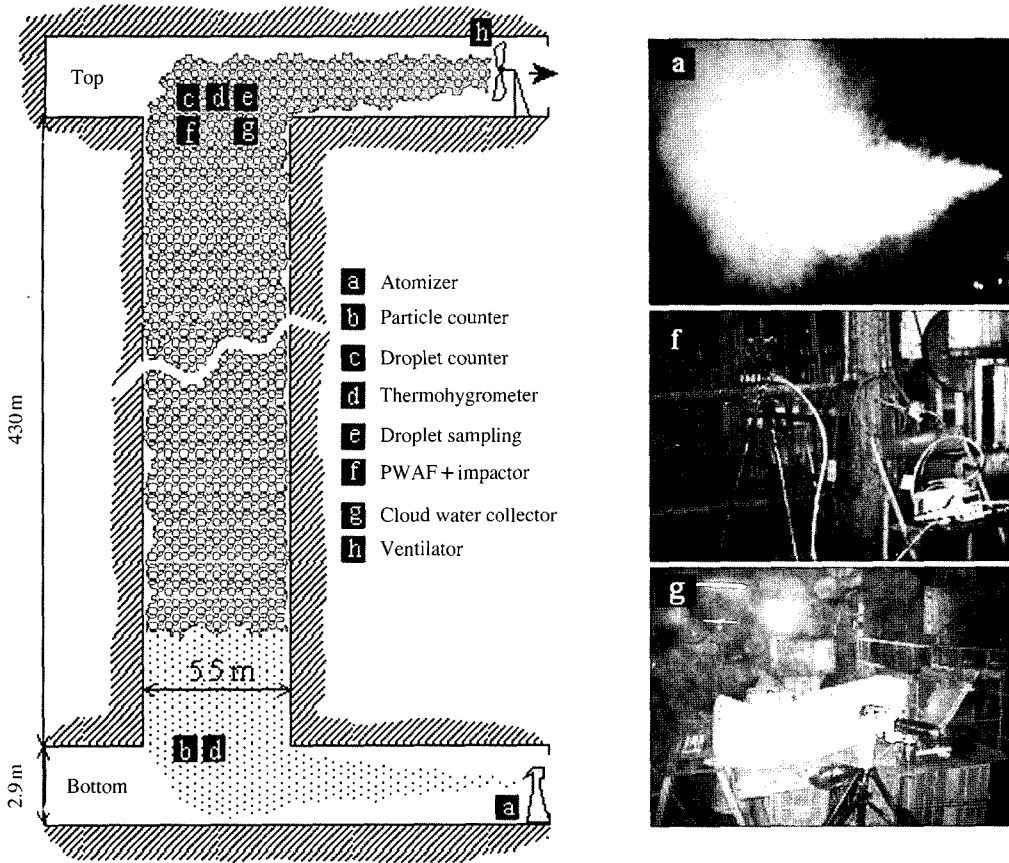


Fig. 1. Schematic illustration of cloud generation at vertical pit (left) and images of aerosol generation (right-top), impactor sampler loading PWF (right-middle) and cloudwater collector (right-bottom).

vertical pit can be calculated to be about 9 minutes. Hence, considering the stability of cloud generation and its moving at the inner vertical pit, the total duration time of each CCN dispersion event was adjusted to 30 minutes. In order to exclude the effect of the former experiment, the atomizer containing NaCl solutions was run at 30 minutes intervals.

The number size distribution of initial dry particles was measured by Scanning Mobility Particle Sizer (SMPS) at bottom site of pit. The number concentration of size-resolved cloud droplets was monitored by Forward Scattering Spectrometer Probe (FSSP) (PMS FSSP-100) at upper site of pit. The SMPS (TSI 3936NL25) consists of the model 3080 classifier and a 3025A-S condensation particle

counter (CPC). And it has the long 3081 DMA which is interchangeable. The SMPS system determines the number concentration of submicrometer aerosols in the range from 10 to 1,000 nm in diameter. Scans are made continuously, so there are no gaps in the data distribution. With 147-size channels and up to 64 channels per size decade, SMPS systems offer the highest accuracy and resolution of any submicrometer-sizing instrument. The scan time of the SMPS is 60 seconds. The SMPS samples aerosol at the rate of 0.3 L min<sup>-1</sup>. Aerosols are sampled directly into the DMA for particle size classification and particle counting by the CPC.

FSSP can fractionate cloud droplets by measuring the amount of light scattered into the collecting

optics aperture during droplet interaction through a focused laser beam. It counts and sizes each individual droplet and thus measures the complete droplet size distribution (Knollenberg, 1981). The standard system sizes droplets from 0.5 to 47  $\mu\text{m}$  diameter in four size ranges. At a sample flow rate of 0.06 L, 6,000 particles per cubic centimeter can be counted with a maximum of a 10% coincidence. The spectra of channel counts are recorded by the probe in a 10 s sampling interval.

The polymeric water absorbent film (PWAf) method developed by Ma *et al.* (2003a) was employed to measure liquid water content ( $W_L$ ) as a function of droplet size. Here, the preparing process of PWAf is briefly explained. Paste phase polymeric solution can be made by agitating the mixture of polymeric water absorbent and pure water. This paste phase solution is mounted on Mylar ( $\text{C}_{10}\text{H}_8\text{O}_4$ ) film. And then it is dried using infrared lamp. Finally PWAf with  $100 \pm 10 \mu\text{m}$  thickness on Mylar film can be obtained and it is setup into the four-stage cascade impactor (Code 8007-3 Sibata Co.) with 1.4, 2.8, 6.4, and 20  $\mu\text{m}$  of 50% cut-off for each stage with a flow rate  $2.71 \text{ min}^{-1}$ . The sampling duration time was 30 minutes in each individual cloud event. The masses of blank PWAf and those of absorbing cloud droplets were measured by an electric microbalance (Sartorius M5P-F) with the lowest detectable mass of 1  $\mu\text{g}$ . More details for making PWAf and size-resolved droplet sampling are described elsewhere (Ma *et al.*, 2003a).

### 2.3 Sampling and analysis of individual droplets

In order to collect individual cloud droplets, the collodion film replication method introduced from Ma *et al.* (2001) was applied. Since the droplet replication process was already described in former studies (Ma *et al.*, 2004; Ma *et al.*, 2003b, c), it was noted here briefly. A viscous collodion solution was mounted onto the Mylar film just before sampling. Cloud droplets adhere onto the thin layer of collodion film, and then they gently settled without bounce-off. After evaporation of alcohol and ether from collodion, a thin film containing the replica-

tions of individual cloud droplets was left. The chemical composition of residual material on droplet replica was determined by micro-Particle Induced X-ray Emission (PIXE).

Micro-PIXE analysis was performed at the division of Takasaki Ion Accelerator for Advanced Radiation Application (TIARA) in Japan Atomic Energy Research Institute (JAERI). Single droplet replica was scanned by 2.6 MeV  $\text{H}^+$  micro beam accelerated by 3 MV single-end accelerator. Beam diameter was 1~2  $\mu\text{m}$ . X-Y beam scanning control signals, which indicate the beam position, are also digitized at the same time. These data are addressed to the 3 D matrices in the memory space, that consist of 1024 channels for the energy spectra and  $128 \times 128$  pixels for corresponding the beam scan area. Beam collection time was about 10~30 min. The more detailed analytical procedures and experimental set-up used for micro-PIXE analysis was described in other publication (Sakai *et al.*, 1998).

## 3. RESULTS AND DISCUSSION

In order to estimate the number size distribution of initial dry particles nebulized by an atomizer, SMPS was operated at the bottom of vertical pit. The dry particles, which acted as CCN particles, were nebulized at one time under the condition of three kinds of solution types. The number size distribution of CCN particles derived from different solution types is displayed in Fig. 2. The initial CCN particles were measured by SMPS at the entrance of vertical pit (see Fig. 1). The monomodal size distributions for every nebulization event of CCN are drawn showing the maximum number level between 70 nm and 90 nm. In the case of background CCN, the peak was formed around 50 nm. In comparison to background particles, the maximum NaCl particle size is shifted to right in proportion to solution concentration. Also the size ranges of particles for the cases of NaCl dry particle nebulization are wider than the case of background particles.

Fig. 3 presents the size spectra of droplet number concentration formed by dry NaCl particles gener-

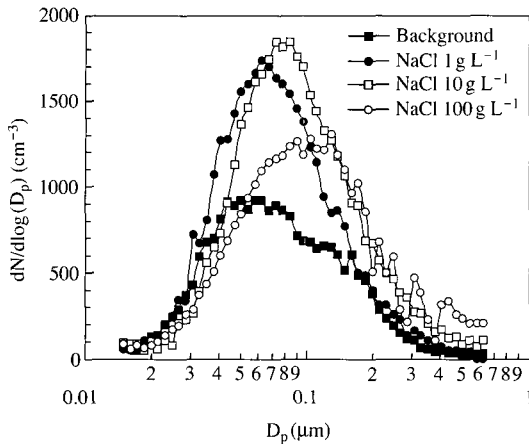


Fig. 2. Number size distribution of background NaCl particles adopted as CCN. The indexed concentration means NaCl solution concentration.

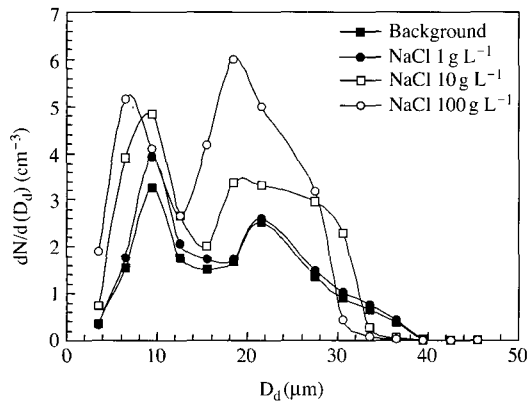


Fig. 3. Size spectra of droplet number concentration formed by different solution types.

ated from three-kind solution types and background particles. This number size distribution of droplets was drawn by the data measured by FSSP at the upper of pit. FSSP monitored the number concentration of size-resolved droplets in each individual event of CCN nebulization. The CCN particle number concentration shows the lognormal form in dependence of the particle size in Fig. 2, while the number size distributions of droplets are bimodal showing the peaks around  $9\ \mu\text{m}$  and  $20\ \mu\text{m}$  for every case. The strong decrease of the droplet number

concentration between  $14\ \mu\text{m}$  and  $16\ \mu\text{m}$  was observed. Also they show the slightly positive skewness with the tail toward larger size. From the droplets spectra, it can be suggested that droplet number concentration strongly depends on the droplet size. Also these spectra suggest that the particle affecting the cloud droplets within the air mass was quite different among the properties of CCN particles. Since the number size distributions of background droplets, which are activated by background mineral particles, are also bimodal, it is suggested that the bimodal distribution has no relevance to the physicochemical properties (i.e. the initial differences in CCN size and particle solubility) of CCN particle.

In general, since the droplets having radii smaller than  $10\ \mu\text{m}$  show little tendency to come together, the coalescence between droplets smaller than  $10\ \mu\text{m}$  cannot occur. Thus, in Fig. 3, the first peak was probably derived from the initial CCN particles shown in Fig. 2 and the valley formed between  $14\ \mu\text{m}$  and  $16\ \mu\text{m}$  and the second peak formed between  $20\ \mu\text{m}$  and  $24\ \mu\text{m}$  may have relevance to the coalescence of droplets around  $14\ \mu\text{m}$  diameter droplets. Since the newly activated droplets, in particular droplets formed by the relatively larger CCN generated during  $\text{NaCl } 100\ \text{g L}^{-1}$  nebulization, are much larger than the pre-existing background ones, the second peaks might be more developed. Hoppel and Fitzgerald (1977) reported that the insoluble component of a particle would need to be 20 times larger than the dry soluble portion in order to affect the equilibrium droplet size at 100% RH. Also the effect of entrainment through a horizontal path connected at upper height of vertical pit can be considered. If the dry air was entrained to clouds, evaporation can occur, but as the parcel rises, tiny droplets grow rapidly as a result of the instant mixing of entrained CCN. Moreover if local environment of the horizontal section ( $5.5\ \text{m}$  by  $2.9\ \text{m}$ ) of vertical pit is a quite dissimilar condition for saturation level, ascending wind speed and external mixing state of background and seed particles, individual droplet have experience quite different growth rates. In the natural atmosphere, in general, a cloud has the

**Table 1. CCN and droplet number concentrations and  $W_L$  in the full size range under each experimental condition.**

	Blank <sup>a</sup>	NaCl 1 g L <sup>-1</sup>	NaCl 10 g L <sup>-1</sup>	NaCl 100 g L <sup>-1</sup>
Number of CCN cm <sup>-3</sup>	22,281	31,811	34,089	37,457
Number of droplet cm <sup>-3</sup>	20	23	29	38
$W_L$ (mg m <sup>-3</sup> )	9.4	10.0	11.3	13.6

<sup>a</sup>When the CCN particles were not nebulized.

number of several hundred per cubic centimeter and having radii of about 10 μm, while the number of droplets counted at this study is only several per cubic centimeter. Precipitation of inner cloud layer can happen by direct collision and coalescence. A small droplet falling through a cloud layer of smaller droplets will collide with only a minute fraction of the droplets in its path. Actually, in the present study, precipitation was visually observed at bottom of pit during the in situ measurement. In general, in the real atmosphere, while the below-cloud scavenging is less efficient than the in-cloud scavenging, aerosol particles are removed by below-cloud scavenging processes during precipitation events (Andronache, 2003).

CCN and droplet number concentrations and  $W_L$  in the full size range under each experimental condition are summarized in Table 1. Both number concentration and  $W_L$  were measured under the condition of 0.8 m s<sup>-1</sup> vertical wind velocity. Remarkably small amount of droplets compared to CCN indicates that a large number of CCN particles were incorporated into cloud droplets. In other words, CCN particles were effectively scavenged by rain out mechanisms. Moreover, the small number of cloud droplets at the top of vertical pit might be driven from the dropping of a large amount of droplets as precipitation as well as scavenging of CCN particles by precipitation.

Fig. 4 displays the schematic view for the life cycle of cloud droplet in the vertical mine chamber. The numbers labeled at both sides mean height scale of vertical pit and time scale of air parcel by fixed updraft velocity, respectively. In the real atmosphere the mechanisms of lift air are orographic lifting, frontal lifting, convergence, and localized convection due to instability, while in the present

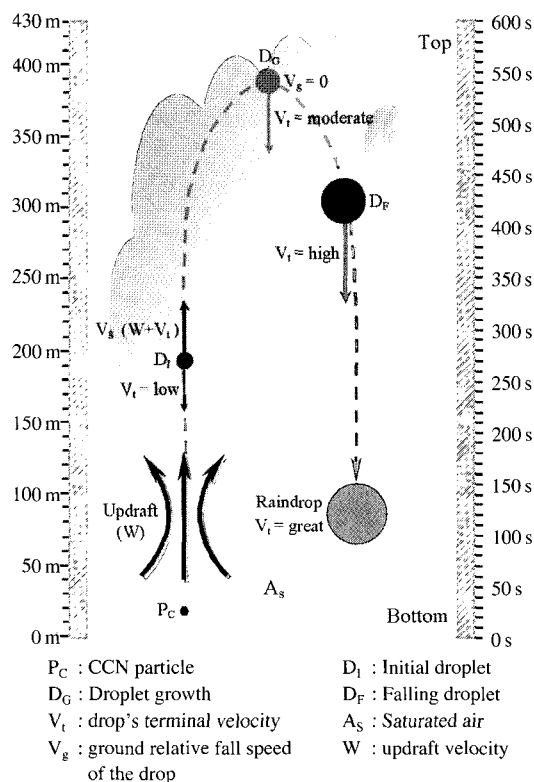


**Fig. 4. Schematic view for the life cycle of cloud droplet in the vertical mine chamber.**

vertical chamber air parcel was ascended (W) by high volume ventilator installed at the top of mine. The introduction of artificial NaCl CCN ( $P_C$ ), formation of initial droplet ( $D_1$ ), condensation growth ( $D_G$ ), and falling droplet ( $D_F$ ) in the vertical transport are important processes that determine the droplet size distribution, droplet number concentration, and  $W_L$  in the vertical fixed environment. And then, cloud droplet number concentration, which is largely determined by how many aerosol

particles are activated as CCN, influences cloud droplet size, liquid water concentration, reflectivity, and precipitation. Here, as one of the most important parameters, the saturated air ( $A_S$ ) determines the potential for droplet growth. Since the particle growth rate is variable according to RH and particle species in the early period of cloud generation (Swietlicki *et al.*, 1999; Zhang *et al.*, 1993; Tang *et al.*, 1977), the different RH should be continuously handled to determine the deliquescence behavior of NaCl particles. However, in the present study, this point cannot be discussed because, as mentioned earlier, the subterranean water of vertical mine makes the mine atmosphere always wet with RH near 100%. At a slight supersaturation, when the RH can become greater than the critical value, the droplet will leave the equilibrium state and grow without limitation by condensation of water vapor. This step ( $D_G$  in Fig. 4) is called activation. In addition, coalescence of these large droplets is responsible for growth of droplets. Large droplets ( $D_F$  in Fig. 4) play a very important role in the initiation of warm rain and their concentration gives an influence on the broadness of the droplet size distribution. (Kuba and Takeda, 1983).

The reason why droplets get big enough to fall can be assume as below. The droplet having several tens of micrometers in diameter is too light to fall out. If one droplet bumps into another droplet, a new bigger droplet will be formed. This is called coalescence. Some droplets will grow large enough to have a terminal velocity ( $V_t$  in Fig. 4) greater than the updraft velocity ( $W$  in Fig. 4) and will start to fall in the cloud. The growing droplet can be called a raindrop as soon as it generally reaches the size of 0.5 mm in diameter or bigger in cumulus cloud at  $4 \text{ m s}^{-1}$  updraft velocity. From the case of natural cumulus cloud, though it cannot be fully evaluated, the size of droplet which starts falling (point  $D_F$  in Fig. 4) will be significantly larger than 0.5 mm diameter because the updraft velocity in the present study was  $0.8 \text{ m s}^{-1}$ .

$W_L$  is one of the most important cloud characteristics for atmospheric chemistry.  $W_L$  of an air parcel starts from almost zero during cloud forma-

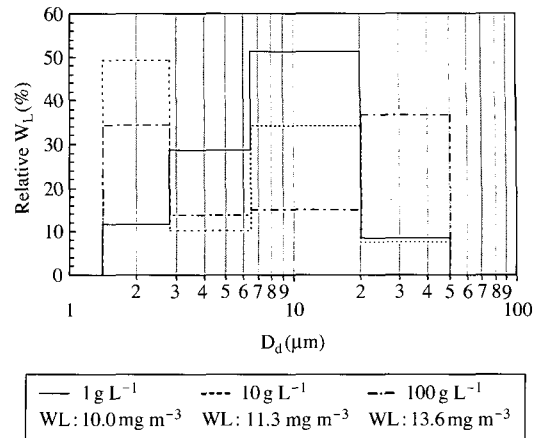


Fig. 5. Droplet size-dependence of  $W_L$  as a function of NaCl solution concentration.

tion, reaches a maximum for a mature cloud, and returns to zero during cloud evaporation. It may considerably vary perpendicularly due to variations in the vertical air velocity. Fig. 5 exhibits the droplet size-dependence of relative  $W_L$  as a function of NaCl solution concentration. This size-resolved droplet  $W_L$  was determined by the PWF method at upper of pit. When NaCl solutions with three-step different concentrations were nebulized, the droplet size resolved  $W_L$  shows the irregular fluctuation across the drop size spectrum independent of total  $W_L$  as shown in Fig. 5. Total  $W_L$  varied from  $10.0 \text{ mg m}^{-3}$  up to  $13.6 \text{ mg m}^{-3}$  with average  $11.6 \text{ mg m}^{-3}$  under the condition of  $0.8 \text{ m s}^{-1}$  vertical wind velocity. As compared with the initial  $W_L$  ( $9.4 \text{ mg m}^{-3}$ ), which measured when the CCN particles were not nebulized, these  $W_L$  levels were continuously increased with increasing of vertical wind velocity. Two types of  $W_L$  distribution are found; a monomodal peak and a bimodal distribution.

Particles in the space of vertical pit are either incorporated into cloud via condensation of water vapor (i.e., heterogeneous nucleation) or due to the uptake of particles by existing droplets. However, particles of unfavorable size and/or composition remain as interstitial particles between the cloud droplets. Thus the mineral particles existing as the background particles in the vertical pit may be exist

as the interstitial particles, which have not been activated to droplets within the cloud. The partitioning of aerosol constituents between cloud droplets and interstitial air plays an important role for the atmospheric residence time of air pollutants. Unfortunately, in the present study, the simultaneous collection and analysis of interstitial particles was not carried out. Therefore the effect of interstitial particles on  $W_L$  for the 4th-stage ( $1.4 \mu\text{m}$  of 50% cut-off) cannot be estimated. However, it can be explained (but inconclusively) that the peaks formed at the 4th-stage (i.e., the peaks shown around  $D_d 2 \mu\text{m}$  in Fig. 5), which causes the bimodal distributions for droplets activated when  $10 \text{ g L}^{-1}$  and  $100 \text{ g L}^{-1}$  NaCl solutions were nebulized, might be driven by the interstitial particles. If these two peaks provably originated from the interstitial particles were excluded from Fig. 5, the result of droplet number concentration shown the maximum around  $10 \mu\text{m}$  and  $20 \mu\text{m}$  in Fig. 3 might draw the monomodal  $W_L$  distribution with the maximum level around  $D_d 20 \mu\text{m}$  in Fig. 5.

NaCl and mineral particles have different chemical property as well as different density. The droplets activated from these two different types of particles will still have unlike density. As the consequence of dissimilar density of CCN particles,  $W_L$  distribution can be fluctuated.

Since  $W_L$  depends not only droplet size but also droplet number concentration, relationship between  $W_L$  and cloud droplet number concentration was investigated. Fig. 6 shows a plot of  $W_L$  versus the number concentration of whole size range droplet.  $W_L$  and whole size range droplet number were measured at top of vertical mine by a cloud water collector ("g" in Fig. 1) and FSSP, respectively. Though  $W_L$  is determined to a large extent by drop size, a good relationship ( $R^2=0.90$ ) between  $W_L$  and cloud droplet number concentration indicate that  $W_L$  can be also determined by droplet number concentration.

Fig. 7 exhibits an example of individual droplet replicas (upper left), Cl map on a single cloud droplet formed under NaCl particle nebulization (upper center), and micro-PIXE spectrum (below).

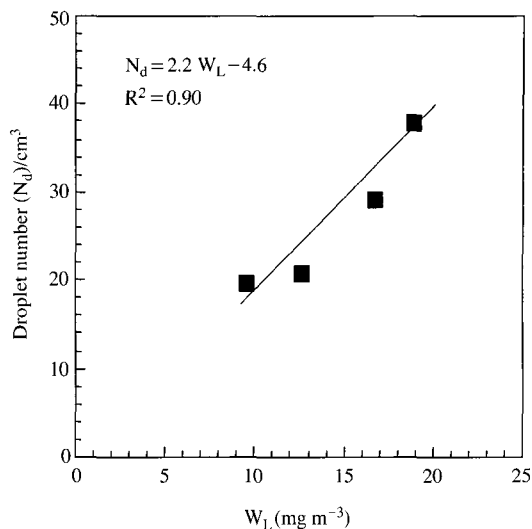


Fig. 6. A plot of  $W_L$  vs. droplet number concentration.

The Fe elemental map is also shown in the right upper corner of Fig. 7. Microbeam scanning area of both elemental maps is  $60 (W) \times 60 (H) \mu\text{m}^2$ . Abscissa and ordinate are pixels corresponding beam scan area. As shown in Fig. 7, the micro-PIXE spectrum and elemental maps were successfully drawn for a single cloud droplet formed. Chlorine with absolutely high peak was distributed on a whole droplet with about  $30 \mu\text{m}$  diameter. Also the NaCl residue with strong X-ray count for Cl is concentrated in the center of elemental map. Both chemical inhomogeneities (mixed components with mineral and Cl) and homogeneities (only mineral components or Cl) in individual droplet replicas were obviously observed from micro-PIXE elemental images. Since the number of single droplet analyzed by micro-PIXE is not enough, though the detail ratio that how many droplets are incorporating NaCl particles (or background mineral particles) cannot be discussed here, it can be suggested that the internal and external mixtures of particles of different chemical composition were at least partly preserved in the droplet phase. Consequently, through the results of micro-PIXE analysis the behavior of CCN particles can be presumed.



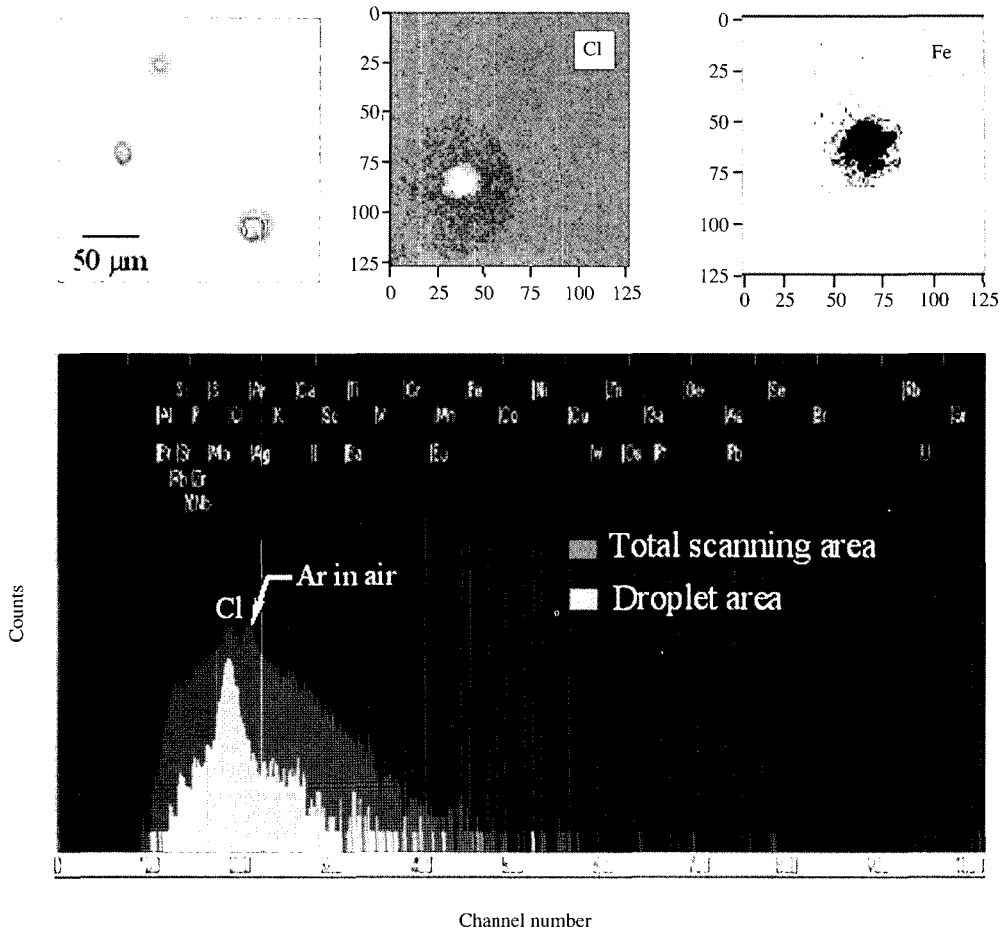


Fig. 7. An example of micro-PIXE spectrum and the elemental maps for Cl and Fe on individual cloud drops.

#### 4. CONCLUSIONS

For the experimental study of cloud properties, the generation of artificial cloud was performed using an extinct vertical mine with 430 m height. Droplet number size distribution was discussed in terms of the water affinity of CCN particles. The liquid water content as a function of droplet size was successfully determined by the polymeric water absorbent film (PWAFF) method. Moreover the chemical properties of individual droplet replicas were determined by micro-PIXE. By a combination of the droplet replication method and micro-PIXE

analytical technique, it was possible to presume the behavior of CCN particles. The number size distributions of cloud droplets indicates that not only the droplet size dependence of droplet number concentration, but also the dissimilarity of particle affecting on cloud droplets within the air mass.  $W_L$  determined by the PWAFF method shows the strong droplet size dependence. Several possible reasons can be considered about the strong droplet size dependence of  $W_L$ . They are the coalescence of droplets, the larger droplets downwards (precipitation falling out of the cloud), the dissimilarity of CCN density, and the mixing of the ascending air parcel with the partial dry air. Though several para-

meters are not in accordance with the real atmosphere, the information obtained from this work should be helpful to better understand the life cycle of cloud and its scavenging processes of aerosol particles.

## ACKNOWLEDGEMENTS

This study was supported in part by funds from the Grant-in-Aid for Scientific Research on Priority Areas under Grant No. 14048212 and 14048213 from Ministry of Education, Culture, Sports, Science and Technology (MEXT), Japan. Authors thank T. Sakai, JAERI Takasaki for the support of micro-PIXE analysis. The authors wish to express thanks to Professor T. Yamada, Department of Civil Engineering, Chuo University and Professor T. Harimaya, Graduate School of Science, Hokkaido University for their support of cloud water samples and monitoring data for particles and droplets, respectively. Finally, I appreciate all the members of Magic Monkey Project, especially professor Mikio Kasahara, for their experimental support.

## REFERENCES

- Andronache, C. (2003) Changes in aerosol size distribution due to below-cloud scavenging by rainfall, European Aerosol Conference 2003, Aug. 31-Sep. 5, Spain, S467-S468.
- Hoppel, W.A. and J.W. Fitzgerald (1977) Measurements of CCN spectra at low supersaturation in relation to fog formation off the coast of Nova Scotia. Proc. Symp., on Radiation in the atmosphere, Science Press, pp. 62-64.
- Garvey, D.M. (1975) Testing of cloud seeding materials at the cloud simulation and aerosol laboratory, 1971-1973, Journal of Applied Meteorology, 14, 883-890.
- Gurciullo, C.S. and S.N. Pandis (1997) Effects of composition variations in cloud droplet populations on aqueous-phase chemistry. Journal of Geophysical Research, 102, 9375-9385.
- Kim, B.G. and T.Y. Kwon (2006) Aerosol indirect studies derived from the ground-based remote sensings, Journal of Korean Society for Atmospheric Environment, 22(2), 235-247 (in Korean).
- Knollenberg, R.G. (1981) Techniques for probing cloud microstructure. In: Hobbs, P.V. (ed), Clouds, their formation, optical properties and effects, Academic Press, New York, pp.15-91.
- Kuba, N. and T. Takeda (1983) Numerical study of the effect of CCN on the size distribution of cloud droplets, Journal of the Meteorological Society of Japan, 61, 375-387.
- Kwak, N.H., R.H. Kim, and M.S. Hong (1990) A study on the development of one-dimensional time-Dependent cumulus cloud model, Journal of Korean Society for Atmospheric Environment, 6(2), 176-182 (in Korean).
- Lee, I.Y., G. Hänel, and H.R. Pruppacher (1980) A numerical determination of the evolution of cloud drop spectra due to condensation on natural aerosol particles, Journal of Atmospheric Science, 37, 1839-1853.
- Ma, C.-J., M. Kasahara, and S. Tohno (2001) A new approach for characterization of single raindrops, Water, Air and Soil Pollution, 130, 1601-1606.
- Ma, C.-J., M. Kasahara, and S. Tohno (2003a) Application of polymeric water absorbent film to the study of drop size-resolved fog samples, Atmospheric Environment, 37, 3749-3756.
- Ma, C.-J., M. Kasahara, S. Tohno, and T. Sakai (2003b) A replication technique for the collection of individual fog droplets and their chemical analysis using micro-PIXE, Atmospheric Environment, 37, 4679-4686.
- Ma, C.-J., M. Kasahara, S. Tohno, and T. Sakai (2003c) A new attempt to study the particle scavenging properties of individual snow crystals using a replication technique, Journal of Japan Society Atmospheric Environment, 38, 89-99.
- Ma, C.-J., S. Tohno, M. Kasahara, and S. Hayakawa (2004) Determination of the chemical properties of residues retained in individual cloud droplets by XRF microprobe at SPring-8, Nuclear Instruments and Methods in Physics Research, 217, 167-175.
- Ratzel, A.C. and E.J. Constantineau (1990) Aerosol cloud generation experiments. 15th international pyrotechnics seminar.
- Sakai, T., T. Hamano, T. Kamiya, K. Murozono, J. Inoue, S. Matsuyama, S. Iwasaki, and K. Ishii (1998)

- Development of a fast multi-parameter data acquisition system for microbeam analyses, Nuclear Instruments and Methods in Physics Research B, 136, 390-394.
- Swietlicki, E., J. Zhou, O.H. Berg, B.G. Martinsson, G. Frank, S. Cederfelt, U. Dusek, A. Berner, W. Birmili, A. Wiedensohler, B. Yuskiwicz, and K.N. Bower (1999) A closure study of sub-micrometer aerosol particle hygroscopic behavior, Atmospheric Research, 50, 205-240.
- Tang, I.N., H.R. Munkelwitz, and J.G. Davis (1977) Aerosol growth studies-II preparation and growth measurements of monodisperse salt aerosols, Journal of Aerosol Science, 8, 149-159.
- Twomey, S., M. Piepgrass, and T.L. Wolfe (1984) An assessment of the impact of pollution on global cloud albedo, Tellus, 36b, 356-366.
- Zhang, X.Q., H. McMurry, S.V. Hering, and G.S. Casuccio (1993) Mixing characteristics and water content of submicron aerosols measured in Los Angeles and at the Grand Canyon, Atmospheric Environment, 27A, 1593-1607.